

Ultimate sharpness of the tunneling resonance in vertical heterostructures

Georgy Alymov^{1,*} and Dmitry Svintsov¹

¹*Moscow Institute of Physics and Technology (National Research University), Dolgoprudny 141700, Russia*

Heterostructures comprised of two two-dimensional electron systems (2DES) separated by a dielectric exhibit resonant tunneling when the band structures of both systems are aligned. It is commonly assumed that the height and width of the resonant peak in the tunneling current is determined by electron scattering and rotational misalignment of crystal structures of the 2DES. We identify two fundamental factors limiting the maximum height and steepness of the resonance: coupling to contacts and tunnel splitting of energy levels. The upper limit of the tunneling current is the number of electrons available for tunneling times half the tunnel coupling between the 2DES. As a result of a tradeoff between the contact-induced level broadening and contact resistance, the maximum current is only achievable when the coupling to contacts equals the tunnel level splitting. According to our model calculations, the limiting behavior can be observed in double-gated graphene/few-layer hexagonal boron nitride/graphene heterostructures.

I. INTRODUCTION

Tunneling heterostructures based on parallel two-dimensional electron systems (2DES) have numerous applications in electronics and photonics. The most established are the quantum well photodetectors [1] and quantum cascade lasers [2], while rich prospects are anticipated for steep-switching tunneling transistors [3, 4]. From a fundamental viewpoint, experimental studies of tunneling current carry the information about electron-electron scattering [5–8] and correlations [9, 10]. Recent advent of van der Waals heterostructures has considerably enriched the field of tunneling electronics [11–14].

The phenomenon of tunneling resonance between parallel 2DES is at the heart of these applications and fundamental studies, and understanding its ultimate magnitude and steepness plays a critical role. The resonance occurs upon perfect alignment of electron bands in the adjacent 2DES. Under this resonance, the charge carriers can transfer from one 2DES to another with conservation of in-plane momentum \mathbf{k} and energy ϵ . The simplest and most commonly used model predicting the resonant peak in current-voltage curves $J(V)$ is based on Bardeen's transfer Hamiltonian [15]

$$J = \frac{2\pi ge}{\hbar} \int \frac{d^2\mathbf{k}}{(2\pi)^2} (f_{b\mathbf{k}} - f_{t\mathbf{k}}) |v_{tb\mathbf{k}}|^2 \delta(\epsilon_{t\mathbf{k}} - \epsilon_{b\mathbf{k}}), \quad (1)$$

where $f_{b/t\mathbf{k}}$ are the distribution functions in bottom (b) and top (t) layers, $\epsilon_{b/t\mathbf{k}}$ are the respective \mathbf{k} -dependent energy bands, and $v_{tb\mathbf{k}}$ is the tunneling matrix element.

When the emitter and collector bands are aligned, $\epsilon_{t\mathbf{k}} = \epsilon_{b\mathbf{k}}$, the transfer Hamiltonian approach in the form of Fermi's golden rule (1) predicts an infinite current [16]. This divergence is usually cured by incorporating electron scattering [17, 18]. Moreover, the assumed link between the resonance width and height and the inelastic quasiparticle scattering rate γ_{sc} became an experimental tool for studies of electron scattering [5, 8].

The theory of tunneling between parallel 2DES in the form of scattering-broadened Fermi's golden rule cannot be considered satisfactory in the limit of weak scattering. Indeed, an

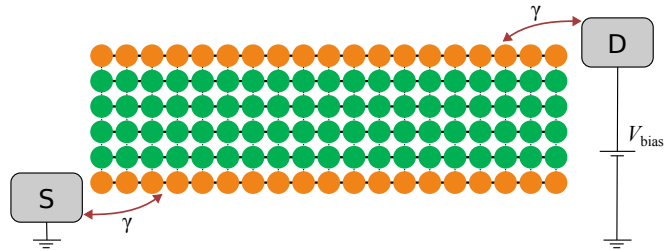


FIG. 1. Schematic of vertical tunneling setup under consideration. Top and bottom two-dimensional systems (orange) are separated by a few-atom thick tunnel barrier (green). The 2DES are connected to the source (S) and drain (D) reservoirs with characteristic carrier exchange rate γ .

electron placed into one of the two tunnel-coupled quantum wells has a finite 'tunneling frequency' $\tau_{\text{tun}}^{-1} = v_{tb\mathbf{k}}/\hbar$. The coherent transfer between the wells cannot be faster than τ_{tun} , thus the resonant current density should be somehow limited by the product of the electron density per layer and the tunneling frequency. At the same time, the tunnel coupling alone cannot result in an interwell dc current, as the electron exhibits coherent beatings between the wells. Only the electron decoherence may interrupt the quantum beatings and lead to a finite current.

In this paper, we analytically address the problem of maximum resonant tunneling current between parallel 2DES, accurately taking into account the tunnel coupling and decoherence induced by the presence of contacts. The experimental setup under consideration is shown in Fig. 1. We analytically show that a combination of these factors determines the ultimate width and height of tunnel resonance even in the absence of disorder and carrier-carrier scattering. We show that even when scattering is negligible, the resonant peak in the tunneling $J(V)$ characteristics still has finite height and width limited by level splitting in the tunnel-coupled emitter and collector and by coupling to the contacts with characteristic rate γ . The resonance height attains its maximum value when these couplings are matched, $\gamma = 2|v_{tb}|$. We rigorously derive a generalization of golden-rule expression for the tunneling current accounting for these effects, and apply it to the experimentally relevant heterostructures comprised of graphene

* alymov@phystech.edu

layers separated by hexagonal boron nitride (hBN). The effects of finite tunnel level splitting on the resonance height and width become pronounced for few-layer hBN barriers even if the graphene layers are rotationally misaligned.

Our derivation is based on the non-equilibrium Green's function formalism in the tight-binding approximation for interlayer coupling [19]. Each 2DES is coupled at its edge to a large electronic reservoir with carrier exchange rate γ . Though similar models have been applied to the transport in van der Waals heterostructures [11, 18, 20–22], the limitations on the resonance width and height imposed by tunnel splitting and coupling to the contacts remained undisclosed. The interplay between coupling to the contacts γ and tunnel coupling is well-studied for quantum dot structures [23–27]. A similar interplay takes place in superlattices [28, 29] and multi-well resonant tunneling diodes with bulk emitters and collectors [30–33]. The non-monotonic dependence of current on the lead-channel coupling γ was also reported in tight-binding simulations of in-plane transport [34, 35].

II. METHODS

A. Model

We consider a heterostructure formed of two 2D materials separated by a dielectric. Hereafter, we will refer to them as top (*t*) and bottom (*b*) leads.

Each lead is coupled to an infinite electron reservoir. In the reservoirs, electrons obey Fermi-Dirac distributions $f_t(E)$, $f_b(E)$ with different chemical potentials μ_t , μ_b . The bottom reservoir is grounded, $\mu_b = 0$, and a bias voltage V_{bias} is applied to the top reservoir, $\mu_t = -eV_{\text{bias}}$.

The (single-particle) Hamiltonian of the whole system is

$$\hat{H} = \begin{pmatrix} \hat{H}_{tt} & \hat{T}_{tr}^\dagger & 0 & 0 & 0 \\ \hat{T}_{tr} & \hat{H}_t & \hat{T}_t^\dagger & 0 & 0 \\ 0 & \hat{T}_t & \hat{H}_d & \hat{T}_b & 0 \\ 0 & 0 & \hat{T}_b^\dagger & \hat{H}_b & \hat{T}_{br} \\ 0 & 0 & 0 & \hat{T}_{br}^\dagger & \hat{H}_{br} \end{pmatrix}, \quad (2)$$

where $\hat{H}_{t(b)}$ is the Hamiltonian of the top (bottom) 2D material, $\hat{H}_{t(b)r}$ is the Hamiltonian of the top (bottom) electron reservoir, \hat{H}_d is the Hamiltonian of the dielectric, and the rest of \hat{H} describes electron hopping between different materials.

B. Green's functions and eigenstates

The retarded Green's function of the system is given by

$$\hat{G}^R = \frac{1}{E - \hat{H} + i0}, \quad (3)$$

and its leads block is

$$\begin{aligned} \hat{G}_l^R &= \begin{pmatrix} \hat{G}_{tt}^R & \hat{G}_{tb}^R \\ \hat{G}_{bt}^R & \hat{G}_{bb}^R \end{pmatrix} \\ &= \begin{pmatrix} E - \hat{H}_t - \hat{v}_{tt} - \hat{\sigma}_t & -\hat{v}_{tb} \\ -\hat{v}_{bt} & E - \hat{H}_b - \hat{v}_{bb} - \hat{\sigma}_b \end{pmatrix}^{-1}, \end{aligned} \quad (4)$$

where $\hat{v}_{ij} = \hat{T}_i^\dagger \hat{g}_d^R \hat{T}_j$ and $\hat{\sigma}_i = \hat{T}_{ir} \hat{g}_d^R \hat{T}_{ir}^\dagger$ are the self-energies due to the lead-dielectric and lead-reservoir coupling, respectively,

and \hat{g}^R denotes the retarded Green's functions of isolated subsystems ($\hat{g}_d^R = \frac{1}{E - \hat{H}_d + i0}$, etc.).

The diagonal terms \hat{v}_{tt} , \hat{v}_{bb} describe the dielectric-induced renormalization of the leads' bandstructures and will be neglected. The tunneling matrix elements \hat{v}_{tb} , \hat{v}_{bt} describe level splitting due to the tunnel coupling between leads. $\hat{v}_{bt} = \hat{v}_{tb}^\dagger$ within the bandgap of the dielectric.

The main role of the reservoirs is to allow electrons to go in and out of the heterostructure, resulting in a finite spectral broadening. We model it with a single scalar quantity γ ($\hat{\sigma}_t = \hat{\sigma}_b = -\frac{i\gamma}{2}$).

In the single band model with electron dispersion relation $\epsilon_{t(b)\mathbf{k}}$ inside the top (bottom) lead and assuming momentum conservation,

$$\hat{G}_{l\mathbf{k}}^R = \frac{1}{(E - \tilde{\epsilon}_{t\mathbf{k}})(E - \tilde{\epsilon}_{b\mathbf{k}}) - |v_{tb\mathbf{k}}|^2} \begin{pmatrix} E - \tilde{\epsilon}_{b\mathbf{k}} & v_{tb\mathbf{k}} \\ v_{bt\mathbf{k}} & E - \tilde{\epsilon}_{t\mathbf{k}} \end{pmatrix}, \quad (5)$$

where \mathbf{k} is the electron momentum, and $\tilde{\epsilon}_{t(b)\mathbf{k}} = \epsilon_{t(b)\mathbf{k}} - \frac{i\gamma}{2}$ are the (complex) electron energies renormalized by interaction with the reservoirs.

$\hat{G}_{l\mathbf{k}}^R(E)$ has poles at energies

$$\begin{aligned} \tilde{\epsilon}_{\pm,\mathbf{k}} &= \epsilon_{\pm,\mathbf{k}} - \frac{i\gamma}{2}, \\ \epsilon_{\pm,\mathbf{k}} &= \frac{\epsilon_{t\mathbf{k}} + \epsilon_{b\mathbf{k}}}{2} \pm \sqrt{\left(\frac{\epsilon_{t\mathbf{k}} - \epsilon_{b\mathbf{k}}}{2}\right)^2 + |v_{tb\mathbf{k}}|^2}, \end{aligned} \quad (6)$$

corresponding to the eigenstates of the tunnel-coupled leads.

C. Tunneling current

The tunneling current can be evaluated using the Landauer-Caroli formula [18, 19, 22, 36]

$$J = \frac{ge}{h} \int \frac{d^2\mathbf{k}}{(2\pi)^2} \int dE (f_b - f_t) \gamma G_{tb\mathbf{k}}^R \gamma G_{bt\mathbf{k}}^A, \quad (7)$$

where g takes into account spin and valley degeneracy.

Putting Green's function (5) into (7), we arrive at

$$\begin{aligned} J &= \frac{ge}{h} \int \frac{d^2\mathbf{k}}{(2\pi)^2} \int dE (f_b - f_t) \gamma^2 \\ &\quad \times \left| \frac{v_{tb\mathbf{k}}}{(E - \epsilon_{+,\mathbf{k}} + \frac{i\gamma}{2})(E - \epsilon_{-,\mathbf{k}} + \frac{i\gamma}{2})} \right|^2 \\ &= \frac{2\pi ge}{\hbar} \int \frac{d^2\mathbf{k}}{(2\pi)^2} \int dE (f_b - f_t) |v_{tb\mathbf{k}}|^2 \\ &\quad \times \Lambda_\gamma(E - \epsilon_{+,\mathbf{k}}) \Lambda_\gamma(E - \epsilon_{-,\mathbf{k}}), \end{aligned} \quad (8)$$

where $\Lambda_\gamma(E) \equiv \frac{1}{\pi} \frac{\gamma/2}{E^2 + \gamma^2/4}$ is a Lorentzian of width γ .

The product $\Lambda_\gamma(E - \epsilon_{+,\mathbf{k}}) \Lambda_\gamma(E - \epsilon_{-,\mathbf{k}})$ has two peaks with equal weights located near $\epsilon_{+,\mathbf{k}}$, $\epsilon_{-,\mathbf{k}}$. If the density of states and the tunneling matrix element do not change significantly on the energy scale of γ (note that the dependence $v_{tb\mathbf{k}}(E)$ in layered materials is not exponential, but power-law [37]), we

can approximate $[f_b(E) - f_t(E)]|v_{tbk}(E)|^2$ by the average of its values at $\epsilon_{\pm,k}$ and integrate over energy analytically:

$$J = \frac{2\pi ge}{\hbar} \int \frac{d^2\mathbf{k}}{(2\pi)^2} (f_{bk} - f_{tk}) |v_{tbk}|^2 \Lambda_{2\gamma}(\epsilon_{+,k} - \epsilon_{-,k}), \quad (9)$$

where $(f_{bk} - f_{tk})|v_{tbk}|^2$ is a shorthand for $\frac{1}{2} \sum_{\pm} [f_b(\epsilon_{\pm,k}) - f_t(\epsilon_{\pm,k})] |v_{tbk}(\epsilon_{\pm,k})|^2$.

When the bandstructures of the top and bottom lead are significantly mismatched, such as in the cases of rotationally misaligned structures, interband tunneling, or leads made of different materials, spectral broadening and energy shifts due to tunnel coupling are usually unimportant, and eq. (9) reduces to the usual Fermi's golden rule

$$J = \frac{2\pi ge}{\hbar} \int \frac{d^2\mathbf{k}}{(2\pi)^2} (f_{bk} - f_{tk}) |v_{tbk}|^2 \delta(\epsilon_{tk} - \epsilon_{bk}). \quad (10)$$

The conditions of its validity are: (i) tunneling is allowed by conservation laws (nonzero current by Fermi's golden rule), (ii) negligible contact resistance ($\gamma \gg |v_{tbk}|$), (iii) negligible spectral broadening (γ is much smaller than the characteristic energy mismatch).

On the other hand, in the case of perfect alignment ($\epsilon_{tk} = \epsilon_{bk}$) Fermi's golden rule predicts infinite current [16–18, 38], while eq. (9) gives a finite answer:

$$\begin{aligned} J &= \frac{2\pi ge}{\hbar} \int \frac{d^2\mathbf{k}}{(2\pi)^2} (f_{bk} - f_{tk}) |v_{tbk}|^2 \Lambda_{2\gamma}(2|v_{tbk}|) \\ &= \frac{ge}{\hbar} \int \frac{d^2\mathbf{k}}{(2\pi)^2} (f_{bk} - f_{tk}) \frac{\gamma}{2} \frac{|v_{tbk}|^2}{|v_{tbk}|^2 + \gamma^2/4}. \end{aligned} \quad (11)$$

Tunneling between perfectly or nearly perfectly aligned bands in van der Waals heterostructures is usually referred to as resonant tunneling [11]. This is a different, but closely related concept to the usual resonant tunneling in double-barrier heterostructures [19].

Equation (11) can be written in a compact form:

$$J = \frac{e}{\hbar} n_{\text{tun}} \frac{\gamma}{2} \frac{|v_{tb}|^2}{|v_{tb}|^2 + \gamma^2/4}, \quad (12)$$

where $|v_{tb}|$ is a suitably averaged tunneling matrix element, and

$$n_{\text{tun}} = g \int \frac{d^2\mathbf{k}}{(2\pi)^2} (f_{bk} - f_{tk}) \quad (13)$$

is the number of electrons participating in tunneling.

The peak current (12) depends on the coupling γ between the leads and reservoirs and vanishes if γ is either very small or very large (blue curve in Fig. 2) [27, 34, 35]. If $\gamma \ll |v_{tb}|$, the lead-reservoir coupling becomes the main bottleneck in electron flow and the current is dominated by the contact resistance. If $\gamma \gg |v_{tb}|$, the spectral weight of electrons becomes spread over a large energy window, thereby reducing the tunneling current.

The tunneling current at the resonance attains its maximum possible value at $\gamma = 2|v_{tb}|$:

$$J_{\max} = e n_{\text{tun}} \frac{|v_{tb}|}{2\hbar}. \quad (14)$$

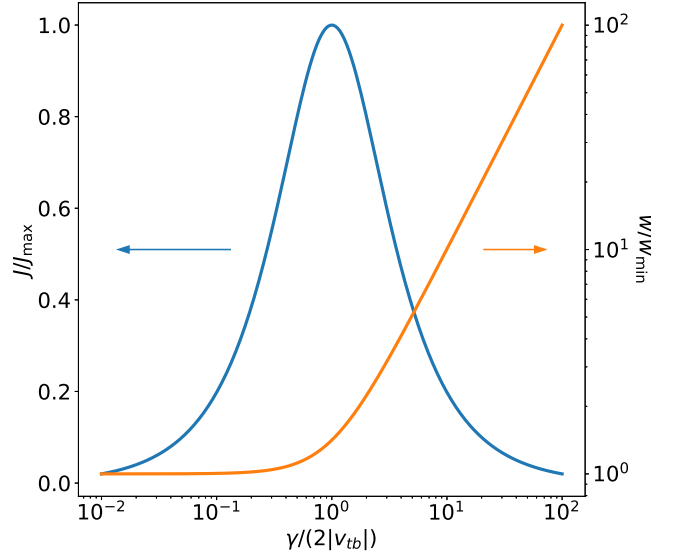


FIG. 2. The height J and width w of the resonant peak in the I - V characteristics of a van der Waals heterostructure vs the coupling to contacts γ in the case of negligible scattering and rotational misalignment. J_{\max} is the maximum possible height, w_{\min} is the minimum possible width, $|v_{tb}|$ is the tunneling matrix element.

In the context of tunneling through quantum dots, this non-monotonic $J(\gamma)$ dependence has been described as a quantum transport analog of Kramers' turnover in the rates of chemical reactions [34, 39] or a manifestation of the quantum Zeno effect [24].

D. Relation to Fermi's golden rule

We have obtained an expression for the height of the resonant peak (12), and now we proceed to calculate its width.

According to eqs. (9) and (6), the tunnel level splitting and coupling to the reservoirs replace the delta function in Fermi's golden rule (10) with a Lorentzian of width $2\sqrt{\gamma^2 + 4|v_{tbk}|^2}$:

$$\begin{aligned} J &= \frac{2\pi ge}{\hbar} \int \frac{d^2\mathbf{k}}{(2\pi)^2} \frac{\gamma}{\sqrt{\gamma^2 + 4|v_{tbk}|^2}} \\ &\times (f_{bk} - f_{tk}) |v_{tbk}|^2 \Lambda_{2\sqrt{\gamma^2 + 4|v_{tbk}|^2}}(\epsilon_{tk} - \epsilon_{bk}). \end{aligned} \quad (15)$$

This spectral broadening translates into a corresponding broadening of the resonant peak, as we will now show for the case of momentum- and energy-independent $|v_{tb}|$.

Suppose the electric potentials of the leads φ_t , φ_b can be controlled by the voltage V_{bias} applied between the leads and/or, in gated structures, by the gate voltage. An external electric field will shift the energies of all electron states in the top (bottom) lead by $U_{t(b)} = -e\varphi_{t(b)}$.

To recover Fermi's golden rule, we insert an auxiliary delta

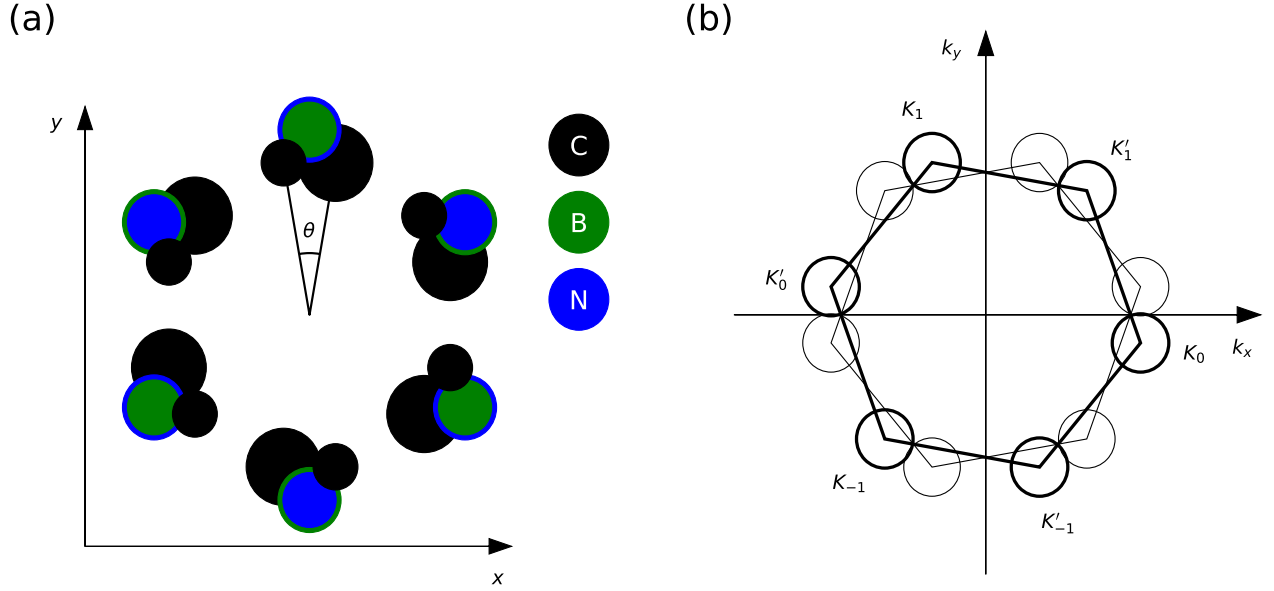


FIG. 3. (a) Relative orientation of the graphene and hBN layers with respect to the chosen coordinate system. Atoms in bottom layers are drawn bigger. (b) Brillouin zones of the top (thin lines) and bottom (thick lines) graphene. Circles illustrate the Fermi surfaces. Labels indicate K and K' valleys; equivalent Dirac cones are numbered with subscripts (index n in eq. (25)). Rotational misalignment and lattice mismatch between graphene and hBN are exaggerated for clarity.

function into (15):

$$J = \frac{\gamma}{\sqrt{\gamma^2 + 4|v_{tb}|^2}} \int d\delta E \Lambda_2 \sqrt{\gamma^2 + 4|v_{tb}|^2} (\delta E) \\ \times \frac{2\pi g e}{\hbar} \int \frac{d^2 \mathbf{k}}{(2\pi)^2} (f_{b\mathbf{k}} - f_{t\mathbf{k}}) |v_{tb}|^2 \delta(\epsilon_{t\mathbf{k}} - \epsilon_{b\mathbf{k}} - \delta E). \quad (16)$$

Now the integrand has almost the form of Fermi's golden rule, except there is an energy mismatch δE and the distribution functions are taken at energies $\epsilon_{\pm\mathbf{k}}$. This can be fixed with appropriate shifts of the leads' bandstructures:

$$\epsilon_{t\mathbf{k},\text{shifted}} = \epsilon_{t\mathbf{k}} - \frac{\delta E}{2} \pm \sqrt{\frac{\delta E^2}{4} + |v_{tb}|^2} = \epsilon_{\pm\mathbf{k}}, \quad (17)$$

$$\epsilon_{b\mathbf{k},\text{shifted}} = \epsilon_{b\mathbf{k}} + \frac{\delta E}{2} \pm \sqrt{\frac{\delta E^2}{4} + |v_{tb}|^2} = \epsilon_{\pm\mathbf{k}}.$$

Thus, the tunneling current J is related to the current J_0 computed via Fermi's golden rule with different electrical potentials of the leads:

$$J(U_t, U_b) = \frac{\gamma}{\sqrt{\gamma^2 + 4|v_{tb}|^2}} \int d\delta E \Lambda_2 \sqrt{\gamma^2 + 4|v_{tb}|^2} (\delta E) \\ \times \frac{1}{2} \sum_{\pm} J_0 \left(U_t - \frac{\delta E}{2} \pm \sqrt{\frac{\delta E^2}{4} + |v_{tb}|^2}, U_b + \frac{\delta E}{2} \pm \sqrt{\frac{\delta E^2}{4} + |v_{tb}|^2} \right). \quad (18)$$

If the current depends on the band alignment much stronger than on the Fermi level, eq. (18) simplifies to

$$J(\Delta U_{tb}) = \frac{\gamma}{\sqrt{\gamma^2 + 4|v_{tb}|^2}} \\ \times \int d\delta E \Lambda_2 \sqrt{\gamma^2 + 4|v_{tb}|^2} (\delta E) J_0(\Delta U_{tb} - \delta E), \quad (19)$$

where $\Delta U_{tb} = U_t - U_b$. At fixed Fermi energies E_{Ft} , E_{Fb} in the leads, $\Delta U_{tb} = -eV_{\text{bias}} - E_{Ft} + E_{Fb}$.

Therefore, the tunneling I - V curves can be obtained from Fermi's golden rule calculations by convolving the results with a Lorentzian of width $2\sqrt{\gamma^2 + 4|v_{tb}|^2}/e$ and multiplying them by an extra attenuation factor $\frac{\gamma}{\sqrt{\gamma^2 + 4|v_{tb}|^2}}$. This is especially useful when the Fermi's golden rule results are known analytically.

As a consequence, the width of the resonant peak in the I - V curves is $2\sqrt{\gamma^2 + 4|v_{tb}|^2}/e$ and cannot be smaller than $4|v_{tb}|/e$ —twice the tunnel level splitting (orange curve in Fig. 2).

Equations similar to (12), (15) have been obtained in the context of resonant tunneling through coupled quantum dots [23–26] and superlattices [28, 29]. In the latter case, carriers are provided by excited subbands instead of contacts.

E. Graphene/hBN/graphene heterostructure

To put our results into a practical perspective, we apply the developed theory to a graphene/few-layer hexagonal boron nitride (hBN)/graphene heterostructure. We assume the

graphene layers are rotated symmetrically with respect to the AA'-stacked hBN slab, with rotation angles $\theta_t = \theta/2$ for the top graphene and $\theta_b = -\theta/2$ for the bottom graphene. The coordinate system that we use is illustrated in Fig. 3.

Graphene is described by a Dirac Hamiltonian [40]

$$\hat{H}_{t(b)\nu\mathbf{k}} = \hbar v_{\text{Gr}} (\nu \sigma_x k_{x'} + \sigma_y k_{y'}) + U_{t(b)}, \quad (20)$$

where v_{Gr} is the Dirac velocity in graphene, σ_x, σ_y are the Pauli matrices, \mathbf{k} is the electron momentum measured from the nearest Dirac point, and $\nu = \pm 1$ is the valley index. $k_{x'}, k_{y'}$ are the components of \mathbf{k} in the reference frame aligned with the corresponding graphene layer:

$$\begin{pmatrix} k_{x'} \\ k_{y'} \end{pmatrix} = \begin{pmatrix} \cos \theta_{t(b)} & \sin \theta_{t(b)} \\ -\sin \theta_{t(b)} & \cos \theta_{t(b)} \end{pmatrix} \begin{pmatrix} k_x \\ k_y \end{pmatrix}. \quad (21)$$

A vertical electric field may be present between the graphene layers, which is included in (20) as a potential energy $U_{t(b)}$.

hBN layers are also described by a Dirac Hamiltonian [11, 18]

$$\hat{H}_{d\nu\mathbf{k},ii} = \begin{cases} \begin{pmatrix} \epsilon_B & 0 \\ 0 & \epsilon_N \end{pmatrix}, & i \text{ odd} \\ \begin{pmatrix} \epsilon_N & 0 \\ 0 & \epsilon_B \end{pmatrix}, & i \text{ even} \end{cases} + U_i \quad (22)$$

(for i th layer), where ϵ_B and ϵ_N are the energies of p_z orbitals of boron and nitrogen measured from the Dirac point of graphene. \mathbf{k} dependence is neglected because of the large bandgap. Again, we include potential energy U_i in the vertical electric field.

Hopping between layers i and $i+1$ in AA'-stacked hBN is described by the interlayer hopping Hamiltonian [18, 41]

$$\hat{H}_{d\mathbf{k},i,i+1} = \hat{H}_{d\mathbf{k},i+1,i} = \begin{pmatrix} t_{\text{BN}} & 0 \\ 0 & t_{\text{BN}} \end{pmatrix}. \quad (23)$$

Hopping between the top (bottom) graphene layer and the top (bottom) hBN layer is described by the following Hamiltonians [11, 42–44]:

$$\begin{aligned} \hat{T}_{t,\nu\mathbf{k}\mathbf{k}'}^\dagger &= \frac{1}{3} \sum_{n=-1}^1 (2\pi)^2 \delta(\mathbf{K}_{t,\nu n} + \mathbf{k} - \mathbf{K}_{\text{hBN},\nu n} - \mathbf{k}') \\ &\times \begin{pmatrix} t_{\text{CB}} & t_{\text{CN}} e^{-\frac{2\pi n i}{3}} \\ t_{\text{CB}} e^{\frac{2\pi n i}{3}} & t_{\text{CN}} \end{pmatrix}, \\ \hat{T}_{b,\nu\mathbf{k}\mathbf{k}'}^\dagger &= \frac{1}{3} \sum_{n=-1}^1 (2\pi)^2 \delta(\mathbf{K}_{b,\nu n} + \mathbf{k} - \mathbf{K}_{\text{hBN},\nu n} - \mathbf{k}') \quad (24) \\ &\times \begin{cases} \begin{pmatrix} t_{\text{CB}} & t_{\text{CN}} e^{-\frac{2\pi n i}{3}} \\ t_{\text{CB}} e^{\frac{2\pi n i}{3}} & t_{\text{CN}} \end{pmatrix}, & N \text{ odd,} \\ \begin{pmatrix} t_{\text{CN}} & t_{\text{CB}} e^{-\frac{2\pi n i}{3}} \\ t_{\text{CN}} e^{\frac{2\pi n i}{3}} & t_{\text{CB}} \end{pmatrix}, & N \text{ even,} \end{cases} \end{aligned}$$

where

$$\begin{aligned} \mathbf{K}_{\text{hBN},\nu n} &= \frac{4\pi}{3a_{\text{hBN}}} \begin{pmatrix} \nu \cos \frac{2\pi n}{3} \\ \sin \frac{2\pi n}{3} \end{pmatrix}, \\ \mathbf{K}_{t(b),\nu n} &= \frac{4\pi}{3a_{\text{Gr}}} \begin{pmatrix} \nu \cos \left(\frac{2\pi n}{3} + \nu \theta_{t(b)} \right) \\ \sin \left(\frac{2\pi n}{3} + \nu \theta_{t(b)} \right) \end{pmatrix} \end{aligned} \quad (25)$$

are the momenta corresponding to the K, K' points in the Brillouin zone of hBN and graphene layers.

From eq. (24) it is evident that tunneling conserves lateral momentum, provided (i) all six corners of the Brillouin zone are regarded as inequivalent, (ii) we always choose the same n in both $\hat{T}_{t,\nu\mathbf{k}\mathbf{k}'}$ and $\hat{T}_{b,\nu\mathbf{k}\mathbf{k}'}$ when calculating the tunneling matrix element. The first condition means that we should use $g = 12$ in eq. (9) (twofold spin degeneracy and sixfold valley degeneracy). The latter condition discards Umklapp processes, which may produce additional peaks in the I - V curves [18, 20, 22], but are ignored in this work to simplify discussion.

Before we proceed with the calculations, we will clarify a few technical details.

First, we need to adapt the single-band equation (9) to two-band graphene. The adaptation is rather straightforward: we (i) insert the band indices s_t, s_b where appropriate, (ii) use graphene spinors $\psi_{s_t,\nu\mathbf{k}_t}^\dagger, \psi_{s_b,\nu\mathbf{k}_b}$ when calculating the tunneling matrix element ($v_{tb,s_t s_b \nu\mathbf{k}_t} = \psi_{s_t,\nu\mathbf{k}_t}^\dagger \hat{T}_{t,\nu\mathbf{k}_t,\mathbf{k}_d}^\dagger \hat{g}_{d\mathbf{k}_d}^R \hat{T}_{b,\nu\mathbf{k}_d,\mathbf{k}_b} \psi_{s_b,\nu\mathbf{k}_b}$), and (iii) sum over bands when calculating the total tunneling current. This is justified because the tunnel coupling between electron states is typically pairwise (at each momentum, tunneling occurs mostly between the two bands that are the closest in energy).

Second, interpreting the results is easier with a constant v_{tb} , while it actually depends on the momentum direction. Thus, we use $|v_{tb\mathbf{k}}|^2$ averaged over the parts of the Brillouin zone where either $\epsilon_{t\mathbf{k}}$ or $\epsilon_{b\mathbf{k}}$ lies between the Fermi levels of the leads.

Third, if the twist angle θ is exactly zero, three possible tunneling paths for each electron (different terms in eq. (24)) end in the same state and interfere with each other. We avoid this special case by using an infinitesimal θ instead of $\theta = 0$ when dealing with perfectly aligned heterostructures.

We use the following values for the model parameters: lattice constant of graphene $a_{\text{Gr}} = 0.2461$ nm [45], lattice constant of hBN $a_{\text{hBN}} = 0.2505$ nm [46], Dirac velocity in graphene $v_{\text{Gr}} = 10^6$ m/s, carbon-boron and carbon-nitrogen hopping parameters $t_{\text{CB}} = 0.39$ eV, $t_{\text{CN}} = 0.26$ eV [42]. For the on-site energies at the boron and nitrogen atoms, we use values $\epsilon_B = -\epsilon_N = 3$ eV to match the experimentally measured bandgap of ~ 6 –7 eV [47–54] and band alignment with graphite [50, 55]. Although the direct electronic gap at the K point of hBN (relevant for tunneling) is not as well known as the usually measured optical gap, this uncertainty can be compensated for by an appropriate choice of the interlayer hopping parameter t_{BN} . We set $t_{\text{BN}} = 0.4$ eV to reproduce the experimental dependence of the tunneling current on the number of hBN layers, $J \propto (\frac{1}{50})^{N_{\text{layers}}}$ [56, 57].

III. RESULTS AND DISCUSSION

We use eq. (9) to calculate the tunneling current in a graphene/hBN (2 layers)/graphene/SiO₂ (300 nm)/gate heterostructure at different couplings to contacts γ and misalignment angles θ . Similar heterostructures, but with a 4-layer tunneling barrier were studied experimentally in Ref. 11.

The calculated I - V curves at fixed Fermi energies $E_{Ft} = 0$,

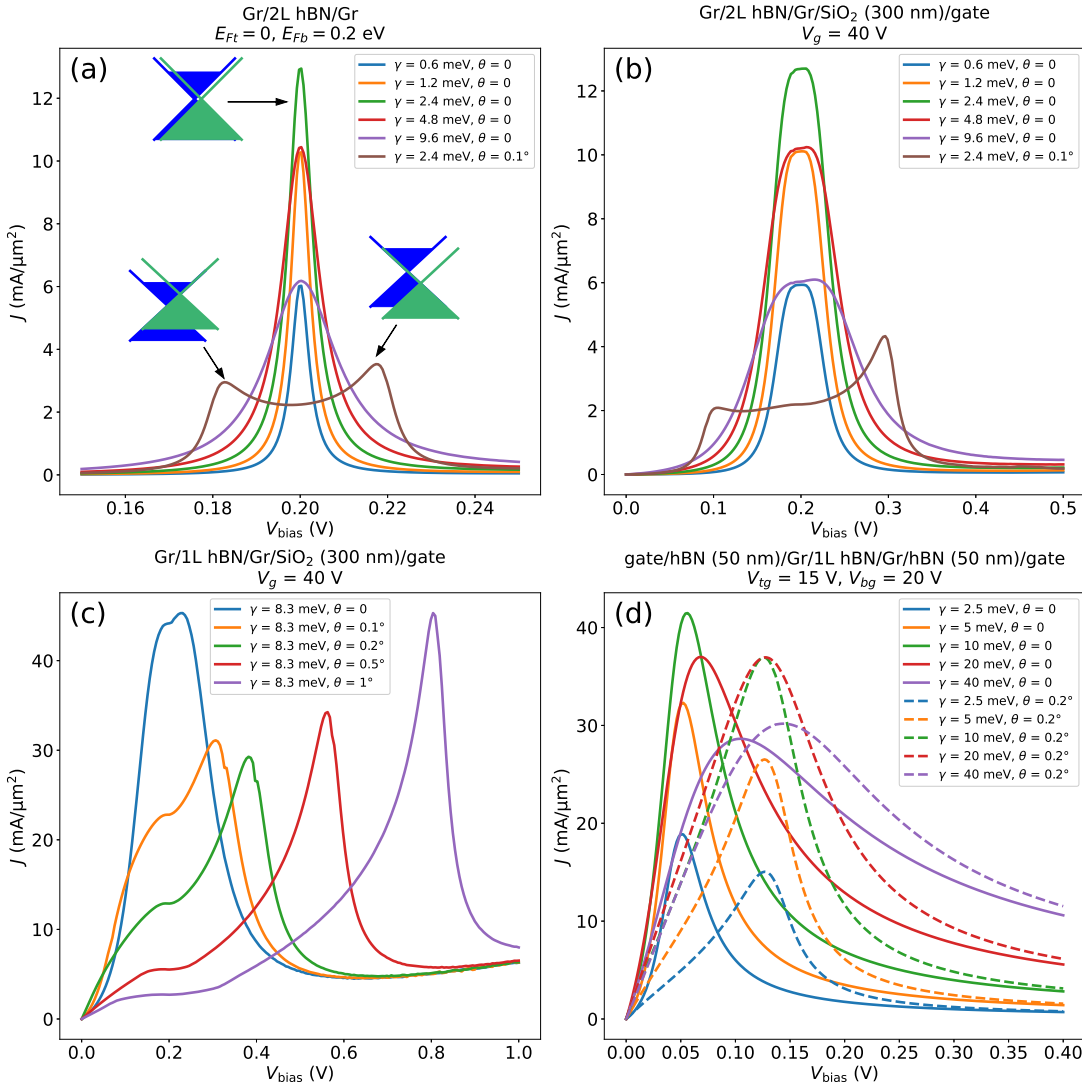


FIG. 4. I - V curves of a graphene/hBN/graphene heterostructure at various couplings to contacts γ and misalignment angles θ . (a) Fixed Fermi energies $E_{Ft} = 0$, $E_{Fb} = 0.2$ eV; (b–c) fixed gate voltage V_g in a single-gated heterostructure; (d) fixed gate voltages V_{tg} , V_{bg} in a double-gated heterostructure. The tunnel barrier is 2 monolayers thick in (a–b) and 1 monolayer thick in (c–d). Insets in (a) show the band alignments corresponding to the resonance conditions with or without rotational misalignment. All the data is for 0 K.

$E_{Fb} = 0.2$ eV are shown in Fig. 4a. We can observe a resonance peak at $V_{\text{bias}} = 0.2$ V, where the Dirac points of both graphenes lie at the same energy.

With two-layer hBN as the tunneling barrier, the average tunneling matrix element $|v_{tb}|$ is 1.2 meV. Therefore, the maximum possible tunneling current is achieved at $\gamma = 2|v_{tb}| = 2.4$ meV (green curve in Fig. 4a). At both smaller and larger γ , the amplitude of the resonance peak is reduced.

The full width at half maximum of the resonance peak is $2\sqrt{4|v_{tb}|^2 + \gamma^2} \approx 4|v_{tb}| = 4.8$ mV at $\gamma \ll 2|v_{tb}|$, slightly increases to $4\sqrt{2}|v_{tb}| = 6.8$ mV at $\gamma = 2|v_{tb}|$ (which maximizes the current), and continues to grow as 2γ at $\gamma \gg 2|v_{tb}|$.

If the graphene layers are doped electrostatically, it is easier to fix the gate voltage than the Fermi energies in individual layers. In this case, the resonance width acquires an extra factor of $f_C = 1 + C_d/C_{qt} + C_d/C_{qb}$, where C_{qt} , C_{qb} are the quantum

capacitances of the graphene layers, and C_d is the classical capacitance of the hBN tunneling barrier [15]. In a single-gated heterostructure, this factor is rather big because the top graphene remains weakly doped and has a small quantum capacitance. This effect is illustrated in Fig. 4b, where I - V curves are calculated at a constant gate voltage of 40 V. At $\gamma = 2.4$ meV (green curve), the peak width is 72 mV—vs 6.8 mV at fixed Fermi energies.

While coupling to the contacts and tunneling-induced level splitting present fundamental limits to the sharpness of the tunneling resonance, in practice there are other factors that contribute to the broadening and attenuation of the resonance peak.

One of these factors is rotational misalignment between the top and bottom graphene. Even a small misalignment of 0.1° is enough to cause a threefold reduction in the maximum current

(brown curves in Figs. 4a, 4b).

Although it makes impossible to achieve perfect band alignment at any V_{bias} , rotational misalignment does not *per se* eliminate the singularity in tunneling current. Tunneling conductance becomes singular not only when the Fermi circles in both leads coincide, but also when they merely touch [17]. Graphene's linear dispersion has a peculiar property: when the Dirac points in the leads are mismatched by ΔU in energy and by \mathbf{q} in momentum, and $\Delta U = \pm \hbar v_{\text{Gr}} q$, then the Fermi circles touch at *every* energy (insets in Fig. 4a). The singularity in conductance survives integration over energy and becomes a square-root singularity in the tunneling current, $J \propto 1/\sqrt{(\hbar v_{\text{Gr}} q)^2 - \Delta U^2}$ [18, 58].

Therefore, rotational misalignment of graphene leads merely splits the resonant delta peak in the tunneling current into two square-root singularities. To obtain a finite current at the “skew resonances” ($\Delta U = \pm \hbar v_{\text{Gr}} q$), we still need to consider the effects of finite γ and v_{tb} .

Using eq. (19), one can derive the following approximate shape of the resonant peaks in the presence of rotational misalignment:

$$J \propto \frac{\gamma}{\gamma_{\text{eff}}} \text{Re} \frac{V_{\text{bias}}}{\sqrt{(\hbar v_{\text{Gr}} q)^2 - \left(\frac{V_{\text{bias}} - V_{\text{res}}}{f_c} + i\gamma_{\text{eff}} \right)^2}}, \quad (26)$$

where $\gamma_{\text{eff}} = \sqrt{\gamma^2 + 4|v_{tb}|^2}$, V_{res} is the resonance position at $\theta = 0$, and we have inserted an extra factor of V_{bias} to get linear behavior at $V_{\text{bias}} \rightarrow 0$.

The dependence of the peak height and width on γ and v_{tb} (dashed curves in Fig. 4d) is similar to the rotationally aligned case (solid curves in Fig. 4d). Of course, the maximum conductance is smaller than in the rotationally aligned case (when *all* electrons with energies between μ_t, μ_b participate in tunneling), but an increase in the rotational misalignment does not always reduce the maximum current (Fig. 4c), although the resonant peak may be shifted outside the experimentally accessible region. This is because the reduction in conductance can be compensated by the increase in the resonant bias voltage, which is significant at large misalignment angles (Fig. 4c).

Another factor contributing to the resonance broadening is electron scattering. Including scattering in calculations is a standard way of obtaining a finite current at the tunneling resonance [16]. There is a number of papers about the effects of static disorder [15, 17, 18, 38, 59], electron-phonon (e-ph) [12, 18], electron-electron (e-e) [21, 60, 61], and electron-plasmon (e-pl) scattering [61] on tunneling characteristics.

Scattering affects the resonant peak in much the same way as coupling to the contacts: compare eq. (12) of this paper with eq. (11) of Ref. 17, eq. (6) of Ref. 60, eq. (9) of Ref. 61, eq. (29) of Ref. 59. To achieve the sharpest possible resonance, the scattering rate γ_{sc} should be less than the tunnel level splitting $2|v_{tb}|$.

Advances in graphene technology make it possible to achieve sub-meV elastic scattering rates [62] (although one should be careful when estimating the quantum lifetime from transport measurements [63, 64]).

Inelastic processes, such as e-e and e-ph scattering, are more difficult to suppress than elastic scattering. Since the resonant

peak is located at a finite V_{bias} , the system is in a nonequilibrium state and can have a significant inelastic scattering rate even at zero temperature. The e-e scattering rate can be estimated as $\gamma_{e-e} \approx \frac{(eV_{\text{bias}})^2}{4\pi E_F} \left[\ln \left(\frac{8E_F}{eV_{\text{bias}}} \right) - \frac{1}{2} \right]$ [65] \approx a few meV or tens of meV for typical values of V_{bias} and E_F [8, 66–68]. The e-ph scattering rate is typically in the sub-meV – few meV range [65, 69].

Therefore, to observe the effect considered in this paper (when the height and width of the tunneling resonance are limited by tunneling itself), a number of conditions must be met: (i) High-quality graphene should be used to minimize the elastic scattering rate. (ii) The resonant peak should be located at small V_{bias} . In this case, the tunneling electrons are close to the Fermi levels of both graphenes, and inelastic scattering is suppressed. (iii) The tunnel barrier must be very thin so that $2|v_{tb}|$ exceeds the scattering rate (\sim a few meV). (iv) Both graphenes must be strongly doped (have a large quantum capacitance) to ensure effective control of band alignment by the bias voltage (i. e., to minimize the f_c factor discussed above). Large Fermi energies also suppress inelastic scattering. (v) The coupling to contacts γ should be close to $2|v_{tb}|$.

Condition (i) favors graphene encapsulated in hBN, which can demonstrate exceptional mobility [62]. Conditions (ii) and (iv) require double gating, which provides independent control over the Fermi energies of both graphenes. Condition (iii) is most easily satisfied with single-layer hBN as the tunnel barrier. Thus, the optimal conditions for observing a resonance whose width is limited by tunnel splitting are realized in a top gate/hBN/graphene/hBN monolayer/graphene/hBN/bottom gate heterostructure.

The calculated I - V curves for such a device are presented in Fig. 4d. The peaks at $\theta = 0$ are significantly narrower than in a similar single-gated heterostructure (Fig. 4c) because of the higher quantum capacitance of the top graphene. However, they are still wider than $2\sqrt{4|v_{tb}|^2 + \gamma^2}$ because the ultrathin barrier has a capacitance comparable to the quantum capacitance of graphene even at large Fermi energies. For example, at $\gamma = 2|v_{tb}| = 10$ meV the peak width is 69 mV instead of $2\sqrt{4|v_{tb}|^2 + \gamma^2} = 28$ mV.

If the misalignment between graphene and hBN is below 1° , an incommensurate-commensurate transition may occur, when graphene lattice spontaneously adapts to hBN lattice and domain walls form at every 14 nm [70]. Note that it does not preclude fabrication of high-quality heterostructures without domain walls where both graphene layers are aligned with each other, but not with hBN. The hBN orientation may affect the barrier height, but the main results of this paper should remain unchanged. In the model we use in this paper, when hBN bands are assumed dispersionless in the lateral directions and Umklapp processes are neglected, the tunneling characteristics do not depend on the hBN orientation at all.

To conclude, we have discussed the effect of the tunneling-induced level shifts and the coupling to contacts on resonant tunneling in van der Waals heterostructures, using a graphene/hBN/graphene heterostructure as an example. We demonstrated that the resonant peak width cannot be less than $4|v_{tb}|$, where v_{tb} is the tunneling matrix

element, and the peak height is maximal when the coupling to contacts γ equals $2|v_{tb}|$. We have shown that these effects can be observed in high-quality double-gated top gate/hBN/graphene/hBN/graphene/hBN/bottom gate heterostructures with ultrathin (1 or 2 monolayers) barriers, when the tunnel coupling exceeds the scattering rate.

ACKNOWLEDGMENTS

This paper is written mostly in GNU TeXmacs [71], a convenient tool for mathematical typesetting.

The work was supported by the grant # 21-79-20225 of the Russian Scientific Foundation.

-
- [1] H. Schneider and H. C. Liu, *Quantum well infrared photodetectors* (Springer, 2007).
- [2] J. Faist, F. Capasso, D. L. Sivco, C. Sirtori, A. L. Hutchinson, and A. Y. Cho, Quantum cascade laser, *Science* **264**, 553 (1994).
- [3] X. Wang, P. Yu, Z. Lei, C. Zhu, X. Cao, F. Liu, L. You, Q. Zeng, Y. Deng, C. Zhu, J. Zhou, Q. Fu, J. Wang, Y. Huang, and Z. Liu, Van der Waals negative capacitance transistors, *Nature Communications* **10**, 3037 (2019).
- [4] X. Xiong, M. Huang, B. Hu, X. Li, F. Liu, S. Li, M. Tian, T. Li, J. Song, and Y. Wu, A transverse tunnelling field-effect transistor made from a van der Waals heterostructure, *Nature Electronics* **3**, 106 (2020).
- [5] S. Q. Murphy, J. P. Eisenstein, L. N. Pfeiffer, and K. W. West, Lifetime of two-dimensional electrons measured by tunneling spectroscopy, *Phys. Rev. B* **52**, 14825 (1995).
- [6] N. Turner, J. T. Nicholls, E. H. Linfield, K. M. Brown, G. A. C. Jones, and D. A. Ritchie, Tunneling between parallel two-dimensional electron gases, *Phys. Rev. B* **54**, 10614 (1996).
- [7] J. Jang, H. M. Yoo, L. N. Pfeiffer, K. W. West, K. W. Baldwin, and R. C. Ashoori, Full momentum- and energy-resolved spectral function of a 2d electronic system, *Science* **358**, 901 (2017).
- [8] N. Prasad, G. W. Burg, K. Watanabe, T. Taniguchi, L. F. Register, and E. Tutuc, Quantum lifetime spectroscopy and magnetotunneling in double bilayer graphene heterostructures, *Phys. Rev. Lett.* **127**, 117701 (2021).
- [9] I. B. Spielman, J. P. Eisenstein, L. N. Pfeiffer, and K. W. West, Resonantly enhanced tunneling in a double layer quantum Hall ferromagnet, *Phys. Rev. Lett.* **84**, 5808 (2000).
- [10] D. Nandi, T. Khaire, A. D. K. Finck, J. P. Eisenstein, L. N. Pfeiffer, and K. W. West, Tunneling at $v_T = 1$ in quantum Hall bilayers, *Phys. Rev. B* **88**, 165308 (2013).
- [11] A. Mishchenko, J. Tu, Y. Cao, R. V. Gorbachev, J. Wallbank, M. Greenaway, V. Morozov, S. Morozov, M. Zhu, S. Wong, F. Withers, C. R. Woods, Y.-J. Kim, K. Watanabe, T. Taniguchi, E. E. Vdovin, O. Makarovsky, T. M. Fromhold, V. I. Fal'ko, A. K. Geim, L. Eaves, and K. S. Novoselov, Twist-controlled resonant tunnelling in graphene/boron nitride/graphene heterostructures, *Nature nanotechnology* **9**, 808 (2014).
- [12] E. E. Vdovin, A. Mishchenko, M. T. Greenaway, M. J. Zhu, D. Ghazaryan, A. Misra, Y. Cao, S. V. Morozov, O. Makarovsky, T. M. Fromhold, A. Patanè, G. J. Slotman, M. I. Katsnelson, A. K. Geim, K. S. Novoselov, and L. Eaves, Phonon-assisted resonant tunneling of electrons in graphene–boron nitride transistors, *Phys. Rev. Lett.* **116**, 186603 (2016).
- [13] M. T. Greenaway, E. E. Vdovin, D. Ghazaryan, A. Misra, A. Mishchenko, Y. Cao, Z. Wang, J. R. Wallbank, M. Hollwill, Y. Khanin, S. V. Morozov, K. Watanabe, T. Taniguchi, O. Makarovsky, T. M. Fromhold, A. Patanè, A. K. Geim, V. I. Fal'ko, K. S. Novoselov, and L. Eaves, Tunnel spectroscopy of localised electronic states in hexagonal boron nitride, *Communications Physics* **1**, 94 (2018).
- [14] J. R. Wallbank, D. Ghazaryan, A. Misra, Y. Cao, J. S. Tu, B. A. Piot, M. Potemski, S. Pezzini, S. Wiedmann, U. Zeitler, T. L. M. Lane, S. V. Morozov, M. T. Greenaway, L. Eaves, A. K. Geim, V. I. Fal'ko, K. S. Novoselov, and A. Mishchenko, Tuning the valley and chiral quantum state of Dirac electrons in van der Waals heterostructures, *Science* **353**, 575 (2016).
- [15] R. M. Feenstra, D. Jena, and G. Gu, Single-particle tunneling in doped graphene-insulator-graphene junctions, *Journal of Applied Physics* **111**, 043711 (2012).
- [16] V. L. Katkov and V. A. Osipov, Review article: Tunneling-based graphene electronics: Methods and examples, *Journal of Vacuum Science & Technology B* **35**, 050801 (2017).
- [17] L. Zheng and A. H. MacDonald, Tunneling conductance between parallel two-dimensional electron systems, *Phys. Rev. B* **47**, 10619 (1993).
- [18] B. Amorim, R. M. Ribeiro, and N. M. R. Peres, Multiple negative differential conductance regions and inelastic phonon assisted tunneling in graphene/h-BN/graphene structures, *Phys. Rev. B* **93**, 235403 (2016).
- [19] S. Datta, *Electronic Transport in Mesoscopic Systems*, Cambridge Studies in Semiconductor Physics and Microelectronic Engineering (Cambridge University Press, 1995).
- [20] L. Brey, Coherent tunneling and negative differential conductivity in a graphene/h-BN/graphene heterostructure, *Phys. Rev. Appl.* **2**, 014003 (2014).
- [21] K. A. Guerrero-Becerra, A. Tomadin, and M. Polini, Resonant tunneling and the quasiparticle lifetime in graphene/boron nitride/graphene heterostructures, *Phys. Rev. B* **93**, 125417 (2016).
- [22] S. Ge, K. M. M. Habib, A. De, Y. Barlas, D. Wickramaratne, M. R. Neupane, and R. K. Lake, Interlayer transport through a graphene/rotated boron nitride/graphene heterostructure, *Phys. Rev. B* **95**, 045303 (2017).
- [23] S. A. Gurvitz, Rate equations for quantum transport in multidot systems, *Phys. Rev. B* **57**, 6602 (1998).
- [24] M. R. Wegewijs and Y. V. Nazarov, Resonant tunneling through linear arrays of quantum dots, *Phys. Rev. B* **60**, 14318 (1999).
- [25] H. Spreeker, G. Kießlich, A. Wacker, and E. Schöll, Coulomb effects in tunneling through a quantum dot stack, *Phys. Rev. B* **69**, 125328 (2004).
- [26] L. Oroszlány, A. Kormányos, J. Kolai, J. Cserti, and C. J. Lambert, Nonthermal broadening in the conductance of double quantum dot structures, *Phys. Rev. B* **76**, 045318 (2007).
- [27] H. K. Yadalam and U. Harbola, Current in nanojunctions: Effects of reservoir coupling, *Physica E: Low-dimensional Systems and Nanostructures* **101**, 224 (2018).
- [28] R. Kazarinov and R. Suris, Electric and electromagnetic properties of semiconductors with a superlattice, *Sov. Phys. Semicond.* **6**, 120 (1972).
- [29] F. Capasso, K. Mohammed, and A. Y. Cho, Sequential resonant tunneling through a multiquantum well superlattice, *Applied Physics Letters* **48**, 478 (1986).
- [30] A. M. Frishman and S. A. Gurvitz, Induced negative conductance in multiple-well heterostructures, *Phys. Rev. B* **47**, 16348 (1993).

- [31] C. A. Stafford and N. S. Wingreen, Resonant photon-assisted tunneling through a double quantum dot: An electron pump from spatial Rabi oscillations, *Phys. Rev. Lett.* **76**, 1916 (1996).
- [32] M. Nagase, K. Furuya, N. Machida, and M. Kurahashi, Current peak characteristics of triple-barrier resonant-tunneling diodes with and without phase breaking, *Japanese Journal of Applied Physics* **40**, 6753 (2001).
- [33] Y. Zohata, T. Nozu, and M. Obara, Resonant tunneling spectroscopy of two coupled quantum wells, *Phys. Rev. B* **39**, 1375 (1989).
- [34] D. Gruss, K. A. Velizhanin, and M. Zwolak, Landauer's formula with finite-time relaxation: Kramers' crossover in electronic transport, *Scientific Reports* **6**, 24514 (2016).
- [35] D. Gruss, A. Smolyanitsky, and M. Zwolak, Communication: Relaxation-limited electronic currents in extended reservoir simulations, *The Journal of Chemical Physics* **147**, 141102 (2017).
- [36] C. Caroli, R. Combescot, P. Nozieres, and D. Saint-James, Direct calculation of the tunneling current, *Journal of Physics C: Solid State Physics* **4**, 916 (1971).
- [37] L. Britnell, R. V. Gorbachev, R. Jalil, B. D. Belle, F. Schedin, A. Mishchenko, T. Georgiou, M. I. Katsnelson, L. Eaves, S. V. Morozov, N. M. R. Peres, J. Leist, A. K. Geim, K. S. Novoselov, and L. A. Ponomarenko, Field-effect tunneling transistor based on vertical graphene heterostructures, *Science* **335**, 947 (2012).
- [38] R. Bistritzer and A. H. MacDonald, Transport between twisted graphene layers, *Phys. Rev. B* **81**, 245412 (2010).
- [39] H. Kramers, Brownian motion in a field of force and the diffusion model of chemical reactions, *Physica* **7**, 284 (1940).
- [40] C. Bena and G. Montambaux, Remarks on the tight-binding model of graphene, *New Journal of Physics* **11**, 095003 (2009).
- [41] R. M. Ribeiro and N. M. R. Peres, Stability of boron nitride bilayers: Ground-state energies, interlayer distances, and tight-binding description, *Phys. Rev. B* **83**, 235312 (2011).
- [42] J. Jung, A. Raoux, Z. Qiao, and A. H. MacDonald, Ab initio theory of moiré superlattice bands in layered two-dimensional materials, *Phys. Rev. B* **89**, 205414 (2014).
- [43] J. R. Wallbank, M. Mucha-Kruczyński, X. Chen, and V. I. Fal'ko, Moiré superlattice effects in graphene/boron-nitride van der Waals heterostructures, *Annalen der Physik* **527**, 359 (2015).
- [44] M. Koshino, Interlayer interaction in general incommensurate atomic layers, *New Journal of Physics* **17**, 015014 (2015).
- [45] L. Jones, Improved crystallographic data for graphite, *Powder diffraction* **18**, 150 (2003).
- [46] W. Paszkowicz, J. Pelka, M. Knapp, T. Szyszko, and S. Podsiadlo, Lattice parameters and anisotropic thermal expansion of hexagonal boron nitride in the 10–297.5 K temperature range, *Applied Physics A* **75**, 431 (2002).
- [47] C. Elias, P. Valvin, T. Pelini, A. Summerfield, C. J. Mellor, T. S. Cheng, L. Eaves, C. T. Foxon, P. H. Beton, S. V. Novikov, B. Gil, and G. Cassabois, Direct band-gap crossover in epitaxial monolayer boron nitride, *Nature Communications* **10**, 2639 (2019).
- [48] G. Cassabois, P. Valvin, and B. Gil, Hexagonal boron nitride is an indirect bandgap semiconductor, *Nature photonics* **10**, 262 (2016).
- [49] S. J. Grenadier, A. Maity, J. Li, J. Lin, and H. Jiang, Effects of unique band structure of *h*-BN probed by photocurrent excitation spectroscopy, *Applied Physics Express* **15**, 051005 (2022).
- [50] R. J. P. Román, F. J. R. C. Costa, A. Zobelli, C. Elias, P. Valvin, G. Cassabois, B. Gil, A. Summerfield, T. S. Cheng, C. J. Mellor, P. H. Beton, S. V. Novikov, and L. F. Zagonel, Band gap measurements of monolayer *h*-BN and insights into carbon-related point defects, *2D Materials* **8**, 044001 (2021).
- [51] M. Hengsberger, D. Leuenberger, A. Schuler, S. Roth, and M. Muntwiler, Dynamics of excited interlayer states in hexagonal boron nitride monolayers, *Journal of Physics D: Applied Physics* **53**, 203001 (2020).
- [52] L. G. Carpenter and P. J. Kirby, The electrical resistivity of boron nitride over the temperature range 700 degrees C to 1400 degrees C, *Journal of Physics D: Applied Physics* **15**, 1143 (1982).
- [53] H. P. R. Frederikse, A. H. Kahn, A. L. Dragoo, and W. R. Hosler, Electrical resistivity and microwave transmission of hexagonal boron nitride, *Journal of the American Ceramic Society* **68**, 131 (1985).
- [54] X. Yang, P. Liu, D. Zhou, F. Gao, X. Wang, S. Lv, Z. Yuan, X. Jin, W. Zhao, H. Wei, L. Zhang, J. Gao, Q. Li, S. Fan, and K. Jiang, High temperature performance of coaxial *h*-BN/CNT wires above 1,000 °C: Thermionic electron emission and thermally activated conductivity, *Nano Research* **12**, 1855 (2019).
- [55] D. Pierucci, J. Zribi, H. Henck, J. Chaste, M. G. Silly, F. Bertran, P. Le Fevre, B. Gil, A. Summerfield, P. H. Beton, S. V. Novikov, G. Cassabois, J. E. Rault, and A. Ouerghi, Van der Waals epitaxy of two-dimensional single-layer *h*-BN on graphite by molecular beam epitaxy: Electronic properties and band structure, *Applied Physics Letters* **112**, 253102 (2018).
- [56] L. Britnell, R. V. Gorbachev, R. Jalil, B. D. Belle, F. Schedin, M. I. Katsnelson, L. Eaves, S. V. Morozov, A. S. Mayorov, N. M. R. Peres, A. H. Castro Neto, J. Leist, A. K. Geim, L. A. Ponomarenko, and K. S. Novoselov, Electron tunneling through ultrathin boron nitride crystalline barriers, *Nano Letters* **12**, 1707 (2012).
- [57] M. Velický, S. Hu, C. R. Woods, P. S. Tóth, V. Zólyomi, A. K. Geim, H. D. Abrúña, K. S. Novoselov, and R. A. W. Dryfe, Electron tunneling through boron nitride confirms Marcus–Hush theory predictions for ultramicroelectrodes, *ACS Nano* **14**, 993 (2020).
- [58] L. Pratley and U. Zülicke, Magnetotunneling spectroscopy of chiral two-dimensional electron systems, *Phys. Rev. B* **88**, 245412 (2013).
- [59] F. T. Vasko, O. G. Balev, and N. Stadart, Inhomogeneous broadening of tunneling conductance in double quantum wells, *Phys. Rev. B* **62**, 12940 (2000).
- [60] T. Jungwirth and A. H. MacDonald, Electron-electron interactions and two-dimensional–two-dimensional tunneling, *Phys. Rev. B* **53**, 7403 (1996).
- [61] D. C. Marinescu, J. J. Quinn, and G. F. Giuliani, Tunneling between dissimilar quantum wells: A probe of the energy-dependent quasiparticle lifetime, *Phys. Rev. B* **65**, 045325 (2002).
- [62] L. Banszerus, M. Schmitz, S. Engels, M. Goldsche, K. Watanabe, T. Taniguchi, B. Beschoten, and C. Stampfer, Ballistic transport exceeding 28 μm in CVD grown graphene, *Nano Letters* **16**, 1387 (2016).
- [63] E. H. Hwang and S. Das Sarma, Single-particle relaxation time versus transport scattering time in a two-dimensional graphene layer, *Phys. Rev. B* **77**, 195412 (2008).
- [64] E. Tiras, S. Ardali, H. Firat, E. Arslan, and E. Ozbay, Substrate effects on electrical parameters of Dirac fermions in graphene, *Materials Science in Semiconductor Processing* **133**, 105936 (2021).
- [65] Q. Li and S. Das Sarma, Finite temperature inelastic mean free path and quasiparticle lifetime in graphene, *Phys. Rev. B* **87**, 085406 (2013).
- [66] S. Gilbertson, T. Durakiewicz, J.-X. Zhu, A. D. Mohite, A. Dattelbaum, and G. Rodriguez, Direct measurement of quasiparticle lifetimes in graphene using time-resolved photoemission, *Journal of Vacuum Science & Technology B* **30**, 03D116 (2012).

- [67] Y. Zeng, J. I. A. Li, S. A. Dietrich, O. M. Ghosh, K. Watanabe, T. Taniguchi, J. Hone, and C. R. Dean, High-quality magnetotransport in graphene using the edge-free Corbino geometry, *Phys. Rev. Lett.* **122**, 137701 (2019).
- [68] C. D. Spataru and F. Léonard, Ab initio calculations of low-energy quasiparticle lifetimes in bilayer graphene, *Applied Physics Letters* **123**, 113101 (2023).
- [69] K. M. Borysenko, J. T. Mullen, E. A. Barry, S. Paul, Y. G. Semenov, J. M. Zavada, M. B. Nardelli, and K. W. Kim, First-principles analysis of electron-phonon interactions in graphene, *Phys. Rev. B* **81**, 121412(R) (2010).
- [70] C. R. Woods, L. Britnell, A. Eckmann, R. S. Ma, J. C. Lu, H. M. Guo, X. Lin, G. L. Yu, Y. Cao, R. Gorbachev, A. V. Kretinin, J. Park, L. A. Ponomarenko, M. I. Katsnelson, Y. Gornostyrev, K. Watanabe, T. Taniguchi, C. Casiraghi, H.-J. Gao, A. K. Geim, and K. Novoselov, Commensurate–incommensurate transition in graphene on hexagonal boron nitride, *Nature Physics* **10**, 451 (2014).
- [71] GNU TeXmacs, <https://www.texmacs.org/>.